ATOMIC-SCALE PROPERTIES OF SEMICONDUCTOR HETEROSTRUCTURES PROBED BY SCANNING TUNNELING MICROSCOPY

E. T. Yu, S. L. Zuo, W. G. Bi, and C. W. Tu

Department of Electrical and Computer Engineering, University of California at San Diego, La Jolla, CA 92093-0407 USA

R. M. Biefeld and A. A. Allerman

Sandia National Laboratories, Albuquerque, NM 87185-0601 USA

Sandia is a multiprogram laboratory operated by Sandia Corporation, a Lockheed Martin Company, for the United States Department of Energy under contract DE-AC04-94AL85000.

The engineering of advanced semiconductor heterostructure materials and devices requires a detailed understanding of, and control over, the structure and properties of semiconductor materials and devices at the atomic to nanometer scale. Cross-sectional scanning tunneling microscopy has emerged as a unique and powerful method to characterize structural morphology and electronic properties in semiconductor epitaxial layers and device structures at these length scales. The basic experimental techniques in cross-sectional scanning tunneling microscopy are described, and some representative applications to semiconductor heterostructure characterization drawn from recent investigations in our laboratory are discussed. Specifically, we describe some recent studies of InP/InAsP and InAsP/InAsSb heterostructures in which nanoscale compositional clustering has been observed and analyzed.

1. INTRODUCTION

The atomic-scale structure of interfaces and alloy layers can exert a profound influence on the electronic, transport, and optical properties of advanced semiconductor heterostructure materials and devices. A detailed understanding of atomic-scale structure, and its relationship to material properties and to various aspects of device performance, is becoming an essential component of semiconductor heterostructure device engineering. Atomic-scale structure of semiconductor heterojunction interfaces, compositional ordering and clustering within semiconductor alloys, discreteness and spatial distribution of dopant atoms, and self-assembly of nanoscale structures can exert a profound influence on material properties and device behavior. The development and effective application of experimental techniques for investigation of such phenomena is, consequently, becoming an endeavor of central importance in research on semiconductor materials and devices.

Recent work by a number of research groups has led to the emergence of cross-sectional scanning tunneling microscopy (STM) as a powerful tool for the investigation

of atomic-scale compositional structure and electronic properties in III-V compound semiconductor heterostructures. The cross-sectional STM technique offers unique capabilities for characterization that, in conjunction with other, complementary experimental techniques are providing new and important insights into material and device properties at the atomic to nanometer scale.[1-8] STM and other scanning probe techniques allow structural, electronic, optical, or other properties of materials and device structures to be characterized directly and with high spatial resolution. These techniques are a powerful complement to many other characterization tools, such as x-ray diffraction, electron diffraction, and electron microscopy, that typically provide less direct information about sample structure and, while offering the ability to probe certain structural or compositional features at the atomic scale, inevitably average these properties over larger areas or volumes.

2. EXPERIMENTAL TECHNIQUE

In cross-sectional STM, a semiconductor wafer is cleaved to expose a cross-section, typically a {110} or {111} plane, of epitaxial layers grown or device structures fabricated on the wafer. Tunneling measurements performed on the exposed cross-sectional surface can then reveal information about the atomic-scale morphology and electronic structure of these epitaxial layers or devices. Figure 1 shows the typical geometry of the sample and STM probe tip in cross-sectional STM; a schematic illustration of the atomic structure of the sample and probe tip near the (110) cleaved surface of a zincblende semiconductor; and a representative, atomically resolved cross-sectional STM image of an InP/InAs$_x$P$_{1-x}$ heterostructure obtained in our laboratory.

As seen in Figure 1, a constant-current image of a semiconductor heterostructure in cross-section will typically exhibit apparent "topographic" contrast between the different materials in the heterostructure, with corrugation amplitudes ranging from less than 0.1nm to over 10nm This contrast is generally ascribed to differences in the electronic properties of the constituent materials rather than to actual physical topography on the cross-sectional surface. Factors such as differing energy band gaps, dopant and carrier concentrations, and electron affinities can contribute to the apparent topographic contrast between materials in a heterostructure. However, variations in band-edge energy from one layer to the next are generally the dominant contributing factor in the observed heterostructure contrast.

DISCLAIMER

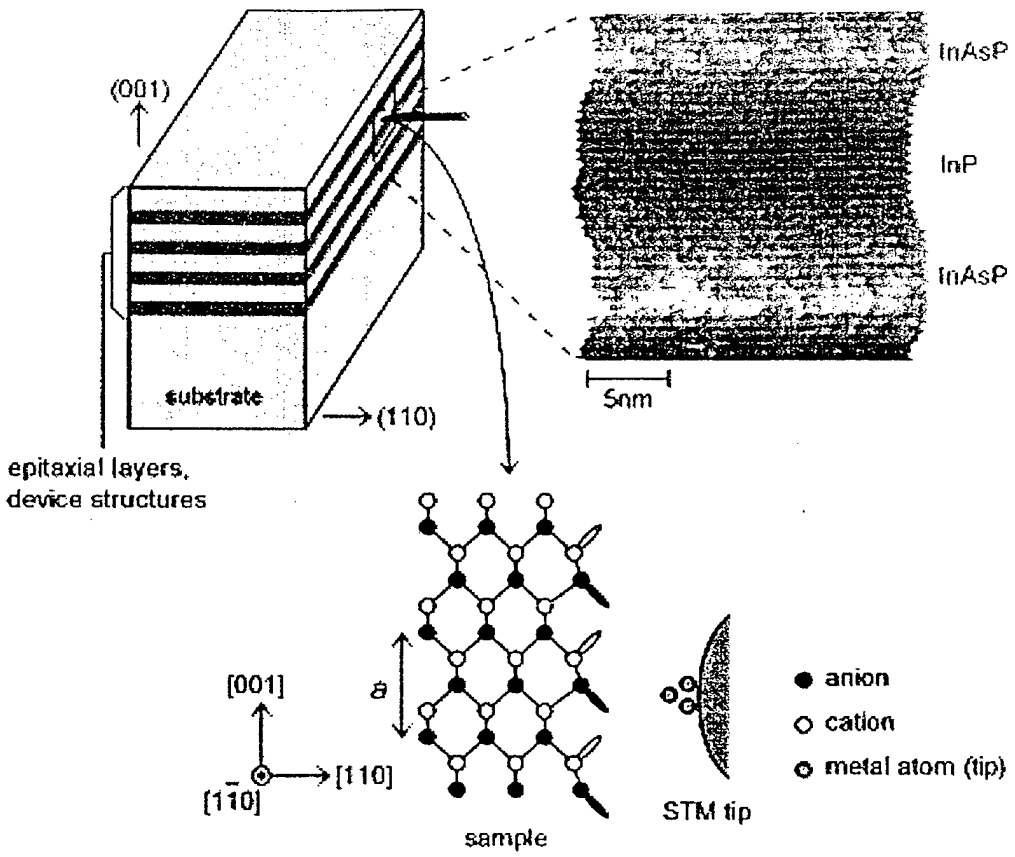

Figure 1. Schematic diagrams of the sample and probe tip geometry in cross-sectional STM and of the arrangement of atoms on the STM tip and on the (110) surface of a zincblende semiconductor, and a representative constant-current image of an InP/InAs$_x$P$_{1-x}$ heterostructure obtained in our laboratory.

3. EXPERIMENTAL RESULTS AND DISCUSSION

The atomic- to nanometer-scale structure of alloy layers and heterojunction interfaces within a semiconductor heterostructure device exerts a marked influence on device performance: atomic-scale interface roughness influences transport in heterojunction field-effect transistors and spectral response in quantum-well-based optoelectronic devices; clustering and ordering within alloys can induce substantial changes in energy band gap; and interface stoichiometry can be a significant factor in determining optical, electronic, and transport properties in mixed-anion heterojunction material systems. A detailed understanding of phenomena such as these, and their relationship to epitaxial crystal growth conditions and to device behavior, plays an essential role in the development of advanced heterostructure devices. Cross-sectional STM can contribute in unique and powerful ways to the development of this understanding. In this section we describe some recent studies of atomic-scale

compositional structure in InP/$InAs_xP_{1-x}$ and $InAs_xP_{1-x}$/$InAs_{1-y}Sb_y$ heterostructures in our laboratory.

InP/$InAs_xP_{1-x}$ heterostructures are emerging as promising materials for optoelectronic devices such as lasers and photodetectors operating at 1.06-1.55μm and for high-speed electronic devices. A very significant issue for $InAs_xP_{1-x}$ and many other ternary and quaternary III-V alloys is the possible presence of ordering, clustering, and/or compositional modulation, phenomena that have been observed to occur in a wide range of material systems[9-11] and that can exert a considerable influence on crystal quality, interface quality, and other electronic as well as optical properties such as band gap, band-edge discontinuities, and carrier transport. Detailed characterization and understanding of these phenomena at the atomic scale are therefore of great importance for optoelectronic and electronic devices based on these materials.

Cross-sectional STM studies of InP/$InAs_xP_{1-x}$ heterostructures have provided insight into the nanoscale compositional structure of $InAs_xP_{1-x}$ alloys and InP/$InAs_xP_{1-x}$ heterojunction interfaces. Samples for these studies were grown by gas-source molecular-beam epitaxy on InP (001) substrates. Figure 2 shows a three-dimensional rendering of a 20nm×20nm constant-current image of a 10nm InP/5nm $InAs_{0.35}P_{0.65}$ multiple-quantum-well structure obtained from a (110) cross-sectional plane at a sample bias of –2.4V and a tunneling current of 0.1nA. Because the valence-band edge of InAs is higher in energy than that of InP, we interpret the brighter features as being associated with As orbitals, and the darker features with P orbitals within the $InAs_{0.35}P_{0.65}$ layer. An asymmetry in interfacial abruptness is apparent, with the $InAs_{0.35}P_{0.65}$-on-InP interface appearing to be relatively abrupt while the InP-on-$InAs_{0.35}P_{0.65}$ interface exhibits greater roughness and compositional grading. In addition, variations in composition at the atomic to nanometer scale are clearly visible, allowing us to investigate in detail the nature and degree of clustering present in the alloy.

Nanoscale As-rich (bright) and P-rich (dark) clusters are clearly seen within the $InAs_{0.35}P_{0.65}$ layer in Figure 2. The figure also shows a magnified view of the $InAs_{0.35}P_{0.65}$ layer, in which we are able to observe that the intersections in the (110) plane of the boundaries between As-rich and P-rich clusters appear to be preferentially oriented along the $[\bar{1}12]$ and $[1\bar{1}2]$ directions in the crystal. The dashed lines in the magnified image delineate a single As-rich cluster within the $InAs_{0.35}P_{0.65}$ alloy. The

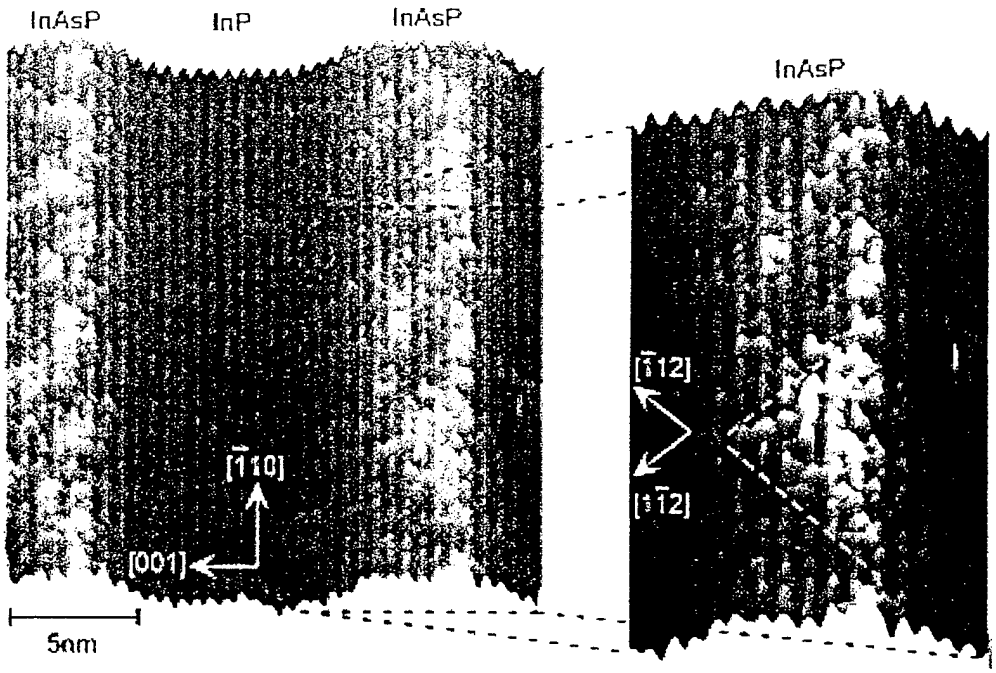

Figure 2. 20nmx20nm filled-state image of the (110) cross section of an InP/$InAs_xP_{1-x}$ heterostructure. Nanoscale compositional clustering within the $InAs_xP_{1-x}$ alloy is clearly visible, with As-rich clusters (bright) appearing to have boundaries in the (110) plane preferentially oriented along the [$\bar{1}$12] and [1$\bar{1}$2] directions.

cluster appears to be approximately triangular in cross-section, with the lower $InAs_{0.35}P_{0.65}$/InP interface constituting a base extending approximately 6-7nm in the [$\bar{1}$10] direction; two sides oriented along the [$\bar{1}$12] and [1$\bar{1}$2] directions form a triangular region approximately 3.5-4nm in height. If we assume that the boundaries between As-rich and P-rich clusters are simple planes, we may deduce from the intersections of the cluster boundaries with the (110) cross-sectional plane that the boundary plane indices (*hkl*) should satisfy the equation $\pm(h-k)+2l=0$, the simplest solutions to which correspond to the ($\bar{1}$11) and (1$\bar{1}$1) planes in the crystal.

Further information about the nanoscale compositional structure of the $InAs_{0.35}P_{0.65}$ alloy layers may be obtained by analysis of cross-sectional images of the (1$\bar{1}$0) plane. Figure 3 shows a three-dimensional rendering of a 40nmx40nm (1$\bar{1}$0) cross-sectional constant-current image of the InP/$InAs_{0.35}P_{0.65}$ heterostructure, obtained at a sample bias of –2.4V and a tunneling current of 0.1nA. A clear asymmetry in interfacial abruptness consistent with that seen in the (110) cross-sectional image is also seen for this orientation. In addition, the $InAs_{0.35}P_{0.65}$ alloy layers show considerably less

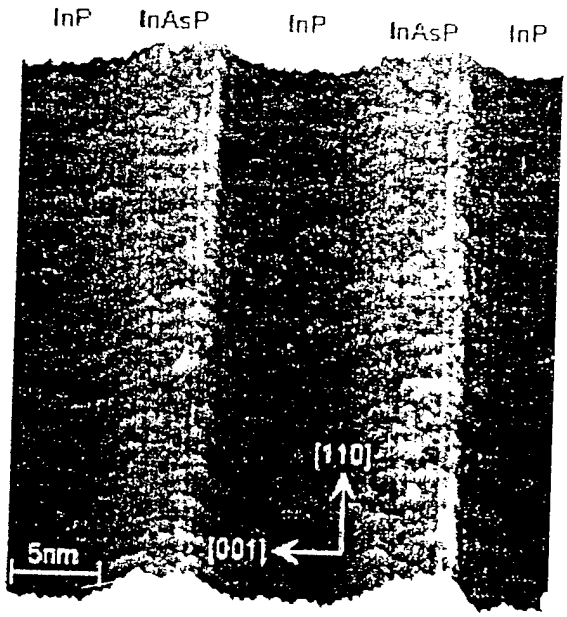

Figure 3. 40nmx40nm filled-state cross-sectional image of the $(1\bar{1}0)$ cross section of an InP/$InAs_{0.35}P_{0.65}$ heterostructure. Less compositional clustering is evident in this image than for the (110) cross-section; compositional features aligned approximately in the [110] direction are observed in the $InAs_{0.35}P_{0.65}$ alloy.

compositional variation along the [110] direction than was evident along the $[\bar{1}10]$ direction in the (110) cross-sectional image. The relatively uniform As composition observed along the [110] lateral direction in the $(1\bar{1}0)$ cross-sectional image combined with the triangular cross-sections of the As-rich and P-rich clusters observed in the (110) image suggests that As-rich and P-rich clusters in the $InAs_{0.35}P_{0.65}$ alloy tend to be elongated along the [110] direction, with roughly triangular cross-sections in the (110) plane.

Nanoscale compositional-clustering is also observed in cross-sectional STM studies of $InAs_{1-x}P_x/InAs_{1-y}Sb_y$ heterostructures grown by metalorganic chemical vapor deposition (MOCVD). $InAs_{1-x}P_x/InAs_{1-y}Sb_y$ strained-layer superlattices have been demonstrated to exhibit excellent performance as materials for light-emitting diodes and lasers operating at wavelengths of 3.2 to 4.4μm.[12,13] Figure 4 shows filled-state cross-sectional images of a 9nm $InAs_{0.73}P_{0.27}$/6.5 nm $InAs_{0.87}Sb_{0.13}$ superlattice grown on an InAs (001) substrate. In contrast to the situation for the InP/$InAs_{0.35}P_{0.65}$ structure discussed above, the $InAs_{0.73}P_{0.27}$ layers in this sample have higher As content than P and are grown under tensile rather than compressive strain. However, there is substantial evidence of nanoscale clustering within the $InAs_{0.73}P_{0.27}$ layer, with the

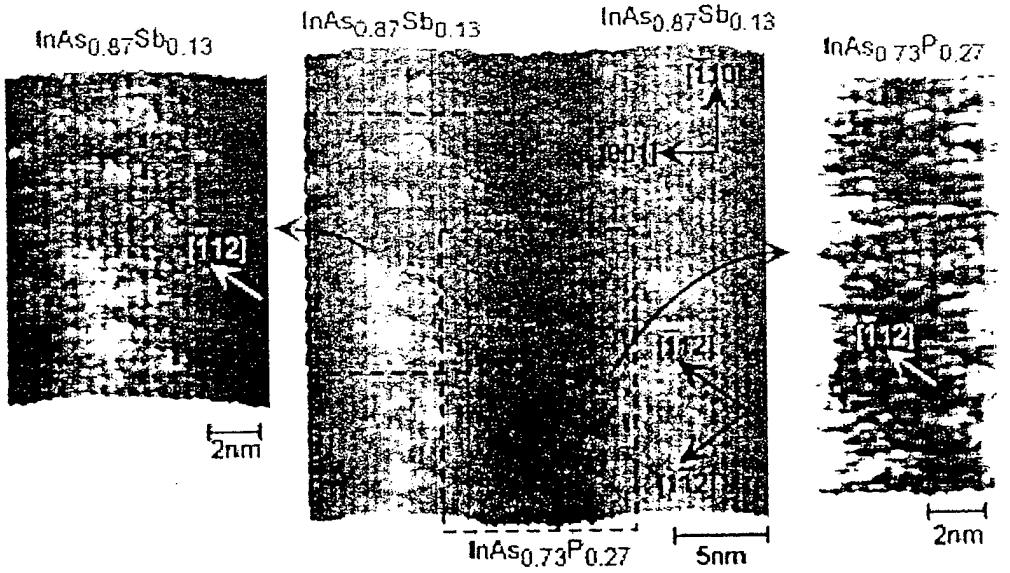

Figure 4. Filled-state (110) cross-sectional images of a 9nm $InAs_{0.73}P_{0.27}$/6.5 nm $InAs_{0.87}Sb_{0.13}$ heterostructure. Nanoscale compositional clustering is observed in both alloy layers, with features appearing to be preferentially aligned along the $[\bar{1}12]$ direction.

boundaries between the As-rich (bright) and P-rich (dark) regions appearing to be oriented preferentially along the $[\bar{1}12]$ direction. Within the $InAs_{0.87}Sb_{0.13}$ layers, nanoscale compositional clustering also appears to occur, with Sb-rich regions appearing bright and As-rich regions dark; a slight degree of preferential alignment of compositional features along the $[\bar{1}12]$ direction appears to be present. These observations are corroborated by electron diffraction studies[14] that have been performed of similarly grown $InAs_{1-y}Sb_y$ alloys: diffraction spots associated with $\{111\}_B$ ordering were observed, with the relative strengths of the two possible $\{111\}_B$ variants, corresponding to ordering along the $[\bar{1}11]$ and $[1\bar{1}1]$ directions, varying with location in the sample. For the region imaged in Figure 4, the observed compositional clustering would correspond to partial ordering along the $[1\bar{1}1]$ direction within both the $InAs_{0.73}P_{0.27}$ and the $InAs_{0.87}Sb_{0.13}$ layers.

4. SUMMARY

Cross-sectional STM has emerged as a powerful technique for probing the properties of advanced semiconductor materials and device structures at the atomic to nanometer scale. The studies described in the preceding sections have illustrated the

ability, using cross-sectional STM, to probe specifically the atomic-scale compositional structure of III-V compound semiconductor alloy layers. These studies are providing information essential for the understanding and optimization of material and device characteristics, and accessible at best indirectly and with considerably less detail by other means. The ability to characterize atomic-scale interface and alloy layer structure in III-V compound semiconductor materials is by now relatively well established, and it is likely that characterization by cross-sectional STM will contribute increasingly to the development and optimization of advanced heterostructure and nanoscale devices in which atomic-scale structure and electronic properties are of paramount importance.

ACKNOWLEDGEMENTS

Part of this work was supported by the National Science Foundation under Award No. ECS 95-01469. One of the authors (E.T.Y.) would like to acknowledge financial support from the Alfred P. Sloan Foundation.

REFERENCES

[1] P. Muralt and D. W. Pohl, *Appl. Phys. Lett.*, **48** (1986) 514.

[2] H. W. M. Salemink, H. P. Meier, R. Ellialtioglu, J. W. Gerritsen, and P. R. M. Muralt, *Appl. Phys. Lett.*, **54** (1989) 1112.

[3] A. R. Smith, S. Gwo, K. Sadra, Y. C. Shih, B. G. Streetman, and C. K. Shih, *J. Vac. Sci. Technol. B*, **12** (1994) 2610.

[4] J. F. Zheng, J. D. Walker, M. B. Salmeron, and E. R. Weber, *Phys. Rev. Lett.*, **72** (1994) 2414.

[5] R. M. Feenstra, D. A. Collins, D. Z.-Y. Ting, M. W. Wang, and T. C. McGill, *Phys. Rev. Lett.*, **72** (1994) 2749.

[6] A. Y. Lew, E. T. Yu, D. H. Chow, and R. H. Miles, *Appl. Phys. Lett.*, **65** (1994) 201.

[7] S. L. Skala, W. Wu, J. R. Tucker, J. W. Lyding, A. Seabaugh, E. A. Beam III, and D. Jovanovic, *J. Vac. Sci. Technol. B*, **13** (1995) 660.

[8] E. T. Yu, *Chem. Rev.*, **97** (1997) 1017.

[9] Y.-E. Ihm, N. Otsuka, J. Klem, and H. Morkoç, *Appl. Phys. Lett.*, **51** (1987) 2013.

[10] H. R. Jen, K. Y. Ma, and G. B. Stringfellow, *Appl. Phys. Lett.*, **54** (1989) 1154.

[11] H. R. Jen, D. S. Cao, and G. B. Stringfellow, *Appl. Phys. Lett.*, **54** (1989) 1890.

[12] S. R. Kurtz, A. A. Allerman, and R. M. Biefeld, *Appl. Phys. Lett.* **70**, 3188 (1997).

[13] R. M. Biefeld, A. A. Allerman, S. R. Kurtz, and J. H. Burkhart, *J. Elec. Mater.* **26**, 1225 (1997).

[14] D. M. Follstaedt, R. M. Biefeld, S. R. Kurtz, and K. C. Baucom, *J. Elec. Mater.* **24**, 819 (1995).

Report Number (14) SAND--98-1035C
CONF-980604--

Publ. Date (11) 199805
Sponsor Code (18) DOE/DP, XF
UC Category (19) UC-700, DOE/ER